NUCLEAR THEORY, Vol. 37 (2018)
eds. M. Gaidarov, N. Minkov, Heron Press, Sofia

Charged-Current Quasielastic (Anti)Neutrino Cross Sections on ^{12}C with Realistic Spectral Functions Including Meson-Exchange Contributions

M.V. Ivanov[1], **A.N. Antonov**[1], **G.D. Megias**[2], **J.A. Caballero**[2], **M.B. Barbaro**[3], **J.E. Amaro**[4], **I. Ruiz Simo**[4], **T.W. Donnelly**[5], **J.M. Udías**[6]

[1]Institute for Nuclear Research and Nuclear Energy, Bulgarian Academy of Sciences, Sofia 1784, Bulgaria
[2]Departamento de Física Atómica, Molecular y Nuclear, Universidad de Sevilla, 41080 Sevilla, Spain
[3]Dipartimento di Fisica, Università di Torino and INFN, Sezione di Torino, Via P. Giuria 1, 10125 Torino, Italy
[4]Departamento de Física Atómica, Molecular y Nuclear, and Instituto de Física Teórica y Computacional Carlos I, Universidad de Granada, Granada 18071, Spain
[5]Center for Theoretical Physics, Laboratory for Nuclear Science and Department of Physics, Massachusetts Institute of Technology, Cambridge, Massachusetts 02139, USA
[6]Grupo de Física Nuclear, Departamento de Estructura de la Materia, Física Aplicada y Electrónica and UPARCOS, Universidad Complutense de Madrid, CEI Moncloa, 28040 Madrid, Spain

Abstract. We present a detailed study of charged-current quasielastic neutrino and antineutrino scattering cross sections on a ^{12}C target obtained using a spectral function that gives a scaling function in accordance with the electron scattering data. The spectral function accounts for the nucleon-nucleon (*NN*) correlations, it has a realistic energy dependence and natural orbitals (NO's) accounting for *NN* correlations from the Jastrow correlation method are used in its construction. The results are compared with those when *NN* correlations are not included, namely when harmonic-oscillator single-particle wave functions are used instead of NO's. A comparison of the results with recent experiments, as well as to results from the superscaling approach is done. The contribution of two-particle two-hole meson-exchange currents on neutrino–nucleus interactions is also considered within a fully relativistic Fermi gas. The results show a good agreement with the experimental data.

1 Introduction

The analysis of neutrino oscillations is at present one of the main research topics in Physics. This explains the huge activity in the field and the numerous exper-

iments that have been proposed in several facilities and covering a very wide range in energy. Recently, the MiniBooNE [1, 2] and T2K [3] collaborations have produced high-quality data, using a mostly carbon target, for a number of selected channels, in particular, for the Quasi-Elastic (QE) one, that is, where no pions are detected in the final state. The treatment of nuclear effects represents one of the main sources of systematic uncertainty in the experimental determination of neutrino oscillation parameters. In particular, the CCQE MiniBooNE results [1, 2] have stimulated many theoretical studies devoted to explaining the apparent discrepancies between the data and most theoretical predictions obtained within the impulse approximation (IA). Based on results from different groups, the inclusion of effects beyond IA, such as multinucleon excitations, mainly two-particle two-hole meson-exchange current (2p-2h MEC) contributions, has allowed one to explain these data without including any effective parameter (such as the axial mass M_A) [4–8].

The aim of the present paper (see also Ref. [9]) is to continue our work from Ref. [10] using the results obtained in Ref. [11] for a realistic spectral function $S(p, \mathcal{E})$ instead of the phenomenological superscaling approximation (SuSA) approach. The spectral function from our previous work [10] will be applied to analysis of CCQE (anti)neutrino cross sections on a ^{12}C target measured by the MiniBooNE [1, 2] and T2K [3] experiments. The new aspect of the present calculation concerns the treatment of 2p-2h excitations. In this work we include the fully relativistic weak (with vector and axial components) charged meson-exchange currents, in both longitudinal and transverse channels. These have been evaluated in [12–14] from an exact microscopic calculation, where the two-body current is the sum of seagull, pion-in-flight, pion-pole, and Δ-pole operators and the basis wave functions are noninteracting Dirac spinors.

2 General Formalism

2.1 Expression for the cross sections

The CC (anti)neutrino-nucleus inclusive cross section in the target laboratory frame can be written in the form (see [15, 16] for details)

$$\left[\frac{d^2\sigma}{d\Omega dk'}\right]_\chi = \sigma_0 \mathcal{F}_\chi^2, \tag{1}$$

where $\chi = +$ for neutrino-induced reactions (in the QE case, $\nu_\ell + n \to \ell^- + p$, where $\ell = e, \mu, \tau$) and $\chi = -$ for antineutrino-induced reactions (in the QE case, $\overline{\nu}_\ell + p \to \ell^+ + n$). The function $\mathcal{F}_\chi^2$ in Eq. (1) depends on the nuclear structure and is presented as a generalized Rosenbluth decomposition [15] containing leptonic kinematical factors, V_K, and five nuclear response functions, R_K, namely VV and AA charge-charge (CC), charge-longitudinal (CL), longitudinal-longitudinal (LL) and transverse (T) contributions, and VA transverse (T') contributions, where $V(A)$ denotes vector(axial-vector) current ma-

trix elements. These are specific components of the nuclear tensor $W^{\mu\nu}$ in the QE region and can be expressed in terms of the superscaling function $f(\psi)$ (see [15] for explicit expressions).

2.2 Models: HO+FSI, NO+FSI, and SuSAv2

In the MiniBooNE experiment the interaction of the neutrino occurs with nucleons bound in nuclei. The analyses of such processes within different methods involve various effects such as nucleon-nucleon (*NN*) correlations, the final state interactions (FSI), possible modifications of the nucleon properties inside the nuclear medium and others. These effects, however, cannot be presently accounted for in an unambiguous and precise way, and what is very important, in most cases they are highly model-dependent. A possible way to avoid the model-dependencies is to use the nuclear response to other leptonic probes, such as electrons, under similar conditions to the neutrino experiments. The SuSA approach follows this general trend. The analyses of superscaling phenomena observed in electron scattering on nuclei have led to the use of the scaling function directly extracted from (e, e') data to predict (anti)neutrino-nucleus cross sections [15], just avoiding the usage of a particular nuclear structure model. A "superscaling function" $f(\psi)$ has been extracted from the data by factoring out the single-nucleon content of the double-differential cross section and plotting the remaining nuclear response versus a scaling variable $\psi(q, \omega)$ (q and ω being the momentum transfer and transferred energy, respectively). For high enough values of the momentum transfer (roughly $q > 400$ MeV/c) the explicit dependence of $f(\psi)$ on q is very weak at transferred energies below the quasielastic peak (scaling of the first kind). Scaling of second kind (*i.e.* no dependence of $f(\psi)$ on the mass number A) turns out to be excellent in the same region. The term "superscaling" means the occurrence of both first and second types of scaling.

In this work we consider three different theoretical calculations. Two of them, denoted as HO (harmonic oscillator) and NO (natural orbitals), make use of a spectral function $S(p, \mathcal{E})$, p being the momentum of the bound nucleon and $\mathcal{E}$ the excitation energy of the residual nucleus, coinciding with the missing energy E_m up to a constant offset [17]. The area of analyses of the scaling function, the spectral function, and their connection (see, *e.g.*, Refs. [11, 18]) provides insight into the validity of the mean-field approximation (MFA) and the role of the *NN* correlations, as well as into the effects of FSI. Though in the MFA it is possible, in principle, to obtain the contributions of different shells to $S(p, \mathcal{E})$ and $n(p)$ for each single-particle state, owing to the residual interactions the hole states are not eigenstates of the residual nucleus but are mixtures of several single-particle states. The latter leads to the spreading of the shell structure and requires studies of the spectral function using theoretical methods going beyond the MFA to describe successfully the relevant experiments. In Ref. [11] a realistic spectral function $S(p, \mathcal{E})$ has been constructed that is in agreement with the scaling function $f(\psi)$ obtained from the (e, e') data. For this

purpose effects beyond MFA have been considered. The procedure included (i) the account for effects of a finite energy spread and (ii) the account for *NN* correlation effects considering single-particle momentum distributions $n_i(p)$ [that are components of $S(p, \mathcal{E})$] beyond the MFA, such as those related to the usage of natural orbitals (NO's) [19] for the single-particle wave functions and occupation numbers within methods in which short-range *NN* correlations are included. For the latter the Jastrow correlation method [20] has been considered. Also, in Ref. [11] FSI were accounted for using complex optical potential that has given a spectral function $S(p, \mathcal{E})$, leading to asymmetric scaling function in accordance with the experimental analysis, thus showing the essential role of the FSI in the description of electron scattering reactions.

In Figure 1 of Ref. [10] the results for the superscaling function $f(\psi)$ within the HO+FSI and NO+FSI models are presented. Accounting for FSI leads to a redistribution of the strength, with lower values of the scaling function at the maximum and an asymmetric shape around the peak position, *viz.,* when $\psi = 0$. Also, we see that the asymmetry in the superscaling function gets larger by using the Lorentzian function for the energy dependence of the spectral function than by using the Gaussian function [10, 11]. The two spectral function models, including FSI, clearly give a much more realistic representation of the data than the relativistic Fermi gas.

The third model, SuSAv2, that is an improved version of the superscaling prescription, called SuSAv2 [21], has been developed by incorporating relativistic mean field (RMF) effects [22–24] in the longitudinal and transverse nuclear responses, as well as in the isovector and isoscalar channels. This is of great interest in order to describe CC neutrino reactions that are purely isovector. Note that in this approach the enhancement of the transverse nuclear response emerges naturally from the RMF theory as a genuine relativistic effect.

The detailed description of the SuSAv2 model can be found in [8, 21, 25]. Here we just mention that it has been validated against all existing (e, e') data sets on ^{12}C, yielding excellent agreement over the full range of kinematics spanned by experiments, except for the very low energy and momentum transfers, where all approaches based on impulse approximation (IA) are bound to fail. Furthermore, the success of the model depends on the inclusion of effects associated with two-body electroweak currents, which will be briefly discussed in the next Section.

2.3 2p-2h MEC contributions

Ingredients beyond the impulse approximation (IA), namely 2p-2h MEC effects, are essential in order to explain the neutrino-nucleus cross sections of interest for neutrino oscillation experiments [5–8, 26, 27]. In particular, 2p-2h MEC effects produce an important contribution in the "dip" region between the QE and Δ peaks, giving rise to a significant enhancement of the impulse approximation responses in the case of inclusive electron- and neutrino-nucleus scattering processes. In this work we make use of the 2p-2h MEC model developed in [13],

which is an extension to the weak sector of the seminal papers [28–30] for the electromagnetic case. The calculation is entirely based on the RFG model, and it incorporates the explicit evaluation of the five response function involved in inclusive neutrino scattering. The MEC model includes one-pion-exchange diagrams derived from the weak pion production model of [31]. This is at variance with the various scaling approaches that are largely based on electron scattering phenomenology, although also inspired in some cases by the RMF predictions.

Following previous works [8, 25, 32, 33], here we make use of a general parametrization of the MEC responses that significantly reduces the computational time. Its functional form for the cases of ^{12}C and ^{16}O is given in [8,25,34], and its validity has been clearly substantiated by comparing its predictions with the complete relativistic calculation.

3 Analysis of Results

In this section we show the predictions of the two spectral function approaches previously described, HO and NO, both including FSI and 2p–2h MEC. We compare the results with data from two different experiments: MiniBooNE and T2K. Our study is restricted to the QE-like regime where the impulse approximation in addition to the effects linked to the 2p-2h meson-exchange currents play the major role. We follow closely the general analysis presented in [8] for the case of the superscaling approach. Hence, for reference, we compare our new theoretical predictions with the results corresponding to the SuSAv2-MEC model.

The predicted ν_μ and $\overline{\nu}_\mu$ fluxes at the MiniBooNE [35] and T2K [36] detectors and corresponding mean energies are compared in Figure 1. $\Phi_{\rm tot}$ is the total integrated ν_μ ($\overline{\nu}_\mu$) flux factor: $\Phi_{\rm tot} = \int \Phi(\epsilon) d\epsilon$, where ϵ is incident beam energy. As observed, the neutrino and antineutrino mean energies correspond-

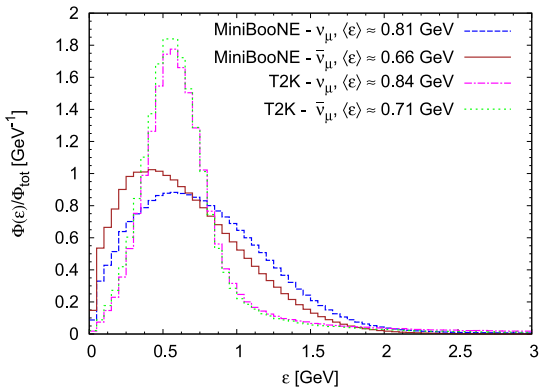

Figure 1. The predicted ν_μ ($\overline{\nu}_\mu$) fluxes at the MiniBooNE [35] and T2K [36] detectors and corresponding mean energies.

ing to MiniBooNE and T2K experiments are rather similar, although the T2K energy flux shows a much narrower distribution. This explains the different role played by 2p-2h MEC effects in the two cases, these being larger for MiniBooNE (see [8] and results in next sections).

3.1 MiniBooNE

In Figures 2 and 3 we show the double differential cross section averaged over the neutrino and antineutrino energy flux against the kinetic energy of the final muon. The data are taken from the MiniBooNE Collaboration [1, 2]. We represent a large variety of kinematical situations where each panel refers to results averaged over a particular muon angular bin.

We compare the data with the results obtained within the HO+FSI, NO+FSI, and SuSAv2 approaches, all of them including 2p–2h MEC, that are also pre-

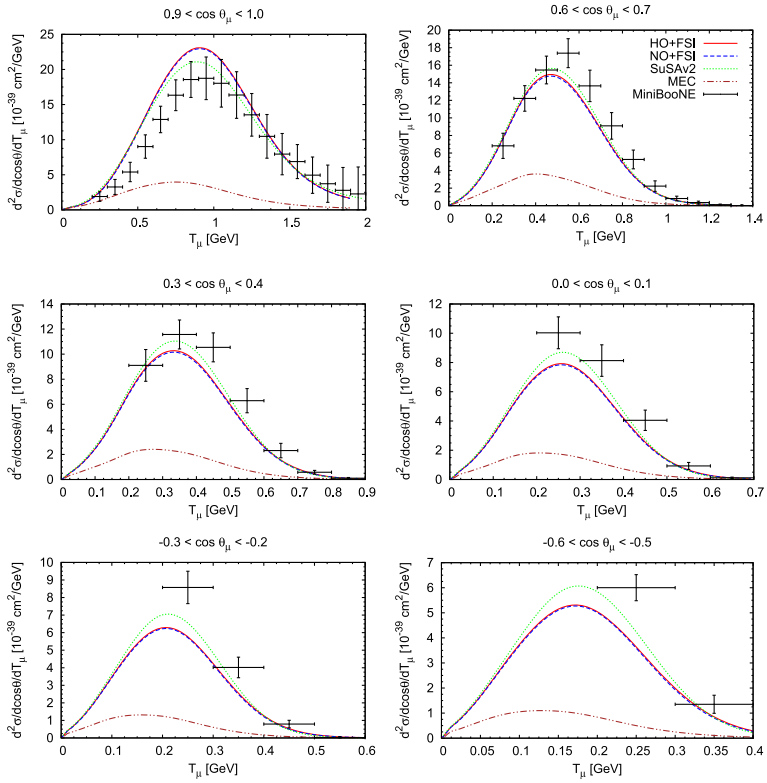

Figure 2. MiniBooNE flux-folded double differential cross section per target neutron for the ν_μ CCQE process on ^{12}C displayed versus the μ^- kinetic energy T_μ for various bins of $\cos\theta_\mu$ obtained within the SuSAv2, HO+FSI, and NO+FSI approaches including MEC. 2p–2h MEC results are also shown separately. The data are from [1].

sented separately. As already shown in [8], we note the relevant role played by 2p-2h MEC contributions, of the order of $\sim$20-25% of the total response at the maximum. In the neutrino case (Figure 2) this relative strength is almost independent of the scattering angle, except for the most forward bin, $0.9 < \cos\theta_\mu < 1$, where the MEC contribution is $\sim$15%; this angular bin, however, largely corresponds to very low excitation energies ($\omega < 50$ MeV) and in this case completely different modeling, appropriate for the near-threshold regime, should be used. In the antineutrino case (Figures 3) the 2p-2h relative strength gets larger for backward scattering angles ($\cos\theta_\mu < -0.2$). This is due to the fact that the antineutrino cross section involves a destructive interference between the T and T' channels and is therefore more sensitive to nuclear effects.

Theoretical predictions including both the QE and the 2p-2h MEC contributions are in good accord with the data in most of the kinematical situations explored. Only at scattering angles approaching 90° and above does one see a

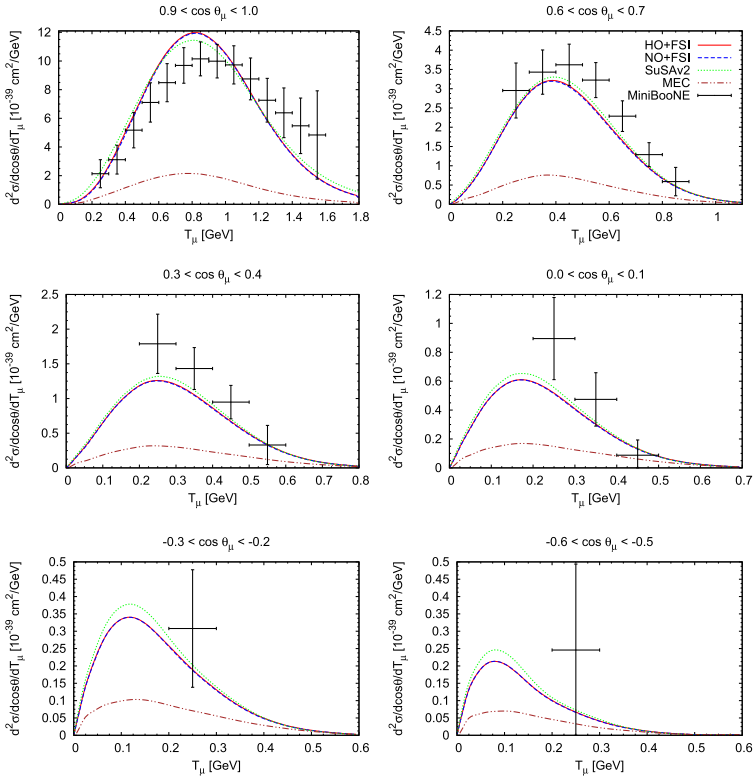

Figure 3. As for Figure 2, but now for the $\overline{\nu}_\mu$ CCQE process on ^{12}C. The data are from [2].

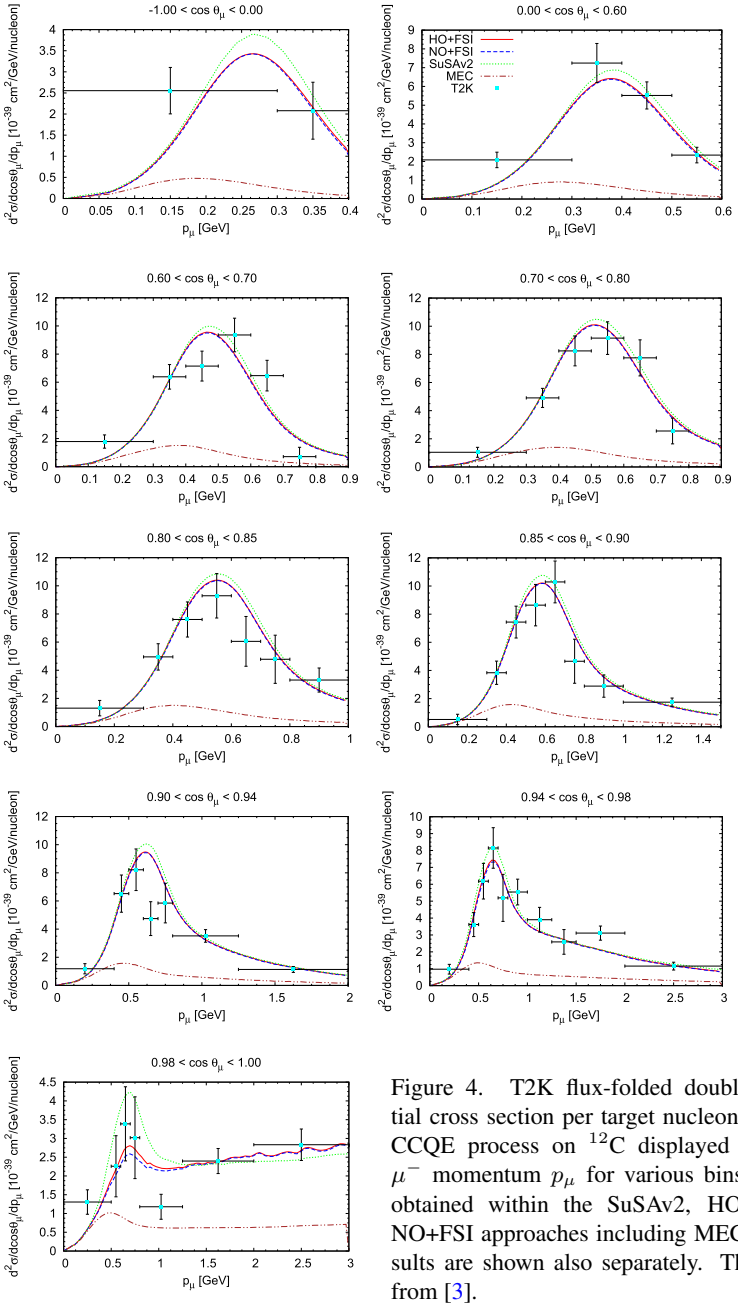

Figure 4. T2K flux-folded double differential cross section per target nucleon for the ν_μ CCQE process on ^{12}C displayed versus the μ^- momentum p_μ for various bins of $\cos\theta_\mu$ obtained within the SuSAv2, HO+FSI, and NO+FSI approaches including MEC. MEC results are shown also separately. The data are from [3].

hint of a difference, although in these situations only a small number of data points with large uncertainties exist.

With regard to the comparison between the different models, we observe that HO+FSI and NO+FSI provide very close responses in all kinematical situations for neutrinos and antineutrinos: the inclusive cross section is not sensitive to the details of the spectral function. Compared with SuSAv2, some differences emerge whose magnitude depends on the scattering angle region explored. Whereas the SuSAv2 prediction is slightly smaller than the SF+FSI one at very forward kinematics (very small energy and momentum transfers), the reverse tends to occur as θ_μ gets larger. Notice that at the most backward kinematics for neutrinos, the SuSAv2 results exceed by $\sim$15% those of the SF+FSI model at the maximum. Similar comments also apply to antineutrinos (Figure 3).

3.2 T2K

In Figure 3.1 we present the flux-averaged double differential cross sections corresponding to the T2K experiment [3]. The graphs are plotted against the muon momentum, and each panel corresponds to a bin in the scattering angle. As in the previous case, we show results obtained within the SuSAv2, HO+FSI, and NO+FSI approaches including MEC and also the separate contributions of the 2p-2h MEC. As already pointed out in [8], the narrower T2K flux, sharply peaked at about 0.7 GeV (see Figure 1), is the reason of the smaller contribution provided by the 2p-2h MEC (of the order of $\sim$10%) as compared with the MiniBooNE results: in fact, the main contribution for the 2p-2h response comes from momentum transfers q $\sim$500 MeV/c, which are less important at T2K kinematics. Concerning the theoretical predictions, the two SF models produce almost identical cross sections that deviate from SuSAv2, particularly at backward kinematics (left-top panel) and very forward scattering (right-bottom panel). At backward angles this is consistent with the analysis presented for the MiniBooNE experiment.

In the particular case of the most forward scattering kinematics (bottom panel on the right), notice that SuSAv2 cross section at the maximum exceeds SF+FSI results by $\sim 30\% - 35\%$. However, the large error bands shown by T2K data do not allow us to discriminate between the different models, *i.e.,* neither between pure QE calculations nor global QE+2p-2h MEC results. Furthermore, notice that the cross section reaches an almost constant value, different from zero, as p_μ increases. This is in contrast with all remaining situations explored in the previous figures.

4 Conclusions

This work extends our previous studies of CCQE neutrino-nucleus scattering processes that are of interest for neutrino (antineutrino) oscillation experiments. Here we focus on models based on the use of two spectral functions, one of them including *NN* short-range correlations through the Jastrow method and,

for a comparison, another without them. Effects of final-state interactions are also incorporated by using an optical potential. These calculations, based on the impulse approximation, are complemented with the contributions given by two-body weak meson exchange currents, giving rise to two-particle two-hole excitations. The model is applied to two different experiments, MiniBooNE and T2K.

These new predictions are compared with the systematic analysis presented in [8] based on the SuSAv2+MEC approach. We find that the spectral function based models (HO+FSI, NO+FSI) lead to results that are very close to the SuSAv2-MEC predictions. Only at the most forward and most backward angles do the differences become larger, being at most of the order of $\sim 10\% - 12\%$. This is in contrast with the contribution ascribed to the 2p-2h MEC effects that can be even larger than $\sim 30\% - 35\%$ compared with the pure QE responses. This proves without ambiguity the essential role played by 2p-2h MEC in providing a successful description of neutrino (antineutrino)-nucleus scattering data for different experiments and a very wide range of kinematical situations.

An interesting outcome of the present study is that the results obtained with the NO spectral function, which accounts for *NN* short-range Jastrow correlations, are very similar to those obtained with the uncorrelated HO spectral function, thus indicating that the role played by this type of correlations is very minor for the observables analyzed in this study. The results in this work can be considered as a test of the reliability of the present spectral function based models. They compare extremely well with the SuSAv2 approach, based on the phenomenology of electron scattering data, although they fail in reproducing neutrino (antineutrino) scattering data unless ingredients beyond the impulse approximation are incorporated. The present study gives us confidence in extending the use of these models to other processes, such as semi-inclusive CCν reactions and neutral current processes.

Acknowledgements

This work was partially supported by the Bulgarian National Science Fund under Contracts Nos. DFNI-T02/19, DFNI-E02/6, and DNTS/Russia 01/3, by the Russian Foundation for Basic Research grant No. 17-52-18057-bolg-a, by the Spanish Ministerio de Economia y Competitividad and ERDF (European Regional Development Fund) under contracts FIS2014-59386-P, FIS2014-53448-C2-1, FIS2017-88410-P, FIS2017-85053-C2-1-P, FPA2015-65035-P, by the Junta de Andalucia (grants No. FQM-225, FQM160), by the INFN under project MANYBODY, by the University of Turin under contract BARM-RILO-17, and part (TWD) by the U.S. Department of Energy under cooperative agreement DE-FC02-94ER40818. GDM acknowledges support from a Junta de Andalucia fellowship (FQM7632, Proyectos de Excelencia 2011). MBB acknowledges support from the "Emilie du Châtelet" programme of the P2IO LabEx (ANR-10-LABX-0038).

References

[1] A.A. Aguilar-Arevalo et al. (MiniBooNE Collaboration), *Phys. Rev. D* **81** (2010) 092005.

[2] A.A. Aguilar-Arevalo et al. (MiniBooNE Collaboration), *Phys. Rev. D* **88** (2013) 032001.

[3] K. Abe et al. (T2K Collaboration), *Phys. Rev. D* **93** (2016) 112012.

[4] M. Martini et al., *Phys. Rev. C* **80** (2009) 065501.

[5] J.E. Amaro et al., *Phys. Lett. B* **696** (2011) 151.

[6] J. Nieves et al., *Physics Letters B* **707** (2012) 72.

[7] O. Lalakulich et al., *Phys. Rev. C* **86** (2012) 014614.

[8] G.D. Megias et al., *Phys. Rev. D* **94** (2016) 093004.

[9] M.V. Ivanov et al., (2018) arXiv:1812.09435 [nucl-th].

[10] M.V. Ivanov et al., *Phys. Rev. C* **89** (2014) 014607.

[11] A.N. Antonov et al., *Phys. Rev. C* **83** (2011) 045504.

[12] I.R. Simo et al., *Phys. Rev. D* **90** (2014) 033012.

[13] I. Ruiz Simo et al., *J. Phys.* **G44** (2017) 065105.

[14] I.R. Simo et al., *Phys. Rev. C* **94** (2016) 054610.

[15] J.E. Amaro et al., *Phys. Rev. C* **71** (2005) 015501.

[16] D.B. Day et al., *Annu. Rev. Nucl. Part. Sci.* **40** (1990) 357.

[17] M. Barbaro et al., *Nuclear Physics A* **643** (1998) 137.

[18] J.A. Caballero et al., *Phys. Rev. C* **81** (2010) 055502.

[19] P.-O. Löwdin, *Phys. Rev.* **97** (1955) 1474.

[20] M.V. Stoitsov, A.N. Antonov, and S.S. Dimitrova, *Phys. Rev. C* **48** (1993) 74.

[21] R. González-Jiménez et al., *Phys. Rev. C* **90** (2014) 035501.

[22] J.A. Caballero et al., *Phys. Rev. Lett.* **95** (2005) 252502.

[23] J.A. Caballero, *Phys. Rev. C* **74** (2006) 015502.

[24] J. Caballero et al., *Physics Letters B* **653** (2007) 366.

[25] G.D. Megias et al., *Phys. Rev. D* **94** (2016) 013012.

[26] T. Katori and M. Martini, *J. Phys. G: Nucl. Part. Phys.* **45** (2018) 013001.

[27] L. Alvarez-Ruso et al., *Prog. Part. Nucl. Phys.* **100** (2018) 1.

[28] J.W. Van Orden and T.W. Donnelly, *Annals Phys.* **131** (1981) 451.

[29] A. De Pace et al., *Nucl. Phys.* **A726** (2003) 303.

[30] J.E. Amaro et al., *Phys. Rev. C* **82** (2010) 044601.

[31] E. Hernández, J. Nieves, and M. Valverde, *Phys. Rev. D* **76** (2007) 033005.

[32] G.D. Megias et al., *Phys. Rev. D* **91** (2015) 073004.

[33] M.V. Ivanov et al., *J. Phys. G: Nucl. Part. Phys.* **43** (2016) 045101.

[34] G.D. Megias et al., (2017) arXiv:1711.00771 [nucl-th].

[35] A.A. Aguilar-Arevalo et al. (MiniBooNE Collaboration), *Phys. Rev. D* **79** (2009) 072002.

[36] K. Abe et al. (T2K Collaboration), *Phys. Rev. D* **87** (2013) 012001.